



*General Features of Hugoniot*

**Los Alamos**  
NATIONAL LABORATORY

*Los Alamos National Laboratory is operated by the University of California  
for the United States Department of Energy under contract W-7405-ENG-36.*

*An Affirmative Action/Equal Opportunity Employer*

*This report was prepared as an account of work sponsored by an agency of the United States Government. Neither The Regents of the University of California, the United States Government nor any agency thereof, nor any of their employees, makes any warranty, express or implied, or assumes any legal liability or responsibility for the accuracy, completeness, or usefulness of any information, apparatus, product, or process disclosed, or represents that its use would not infringe privately owned rights. Reference herein to any specific commercial product, process, or service by trade name, trademark, manufacturer, or otherwise, does not necessarily constitute or imply its endorsement, recommendation, or favoring by The Regents of the University of California, the United States Government, or any agency thereof. The views and opinions of authors expressed herein do not necessarily state or reflect those of The Regents of the University of California, the United States Government, or any agency thereof. The Los Alamos National Laboratory strongly supports academic freedom and a researcher's right to publish therefore, the Laboratory as an institution does not endorse the viewpoint of a publication or guarantee its technical correctness*

*General Features of Hugoniot*

*J. D. Johnson*

# GENERAL FEATURES OF HUGONIOTS

by

J. D. Johnson

## ABSTRACT

From thermodynamics and the Hugoniot jump relations I derive a simple algebraic equation among the Grüneisen constant  $\gamma$ , bulk modulus  $B_s$ , pressure  $P$ , particle velocity  $U_p$ , and slope  $s$  and intercept  $c$  of the tangent line to the  $U_s - U_p$  Hugoniot at  $U_p$ . At  $U_p = 0$ ,  $s$  is simply related to  $\partial B_s / \partial P)_s$  and for  $10 \text{ km/s} \lesssim U_p \lesssim 100 - 200 \text{ km/s}$  there is a very linear region in the  $U_s - U_p$  curve. When  $dP/d\rho = \infty$ ,  $s$  and the curvature are directly given by  $P$ ,  $B_s$  and  $\gamma$ . I end with the excellent confirmation of the linear region in data and with a discussion of shell structure.

## Introduction

There has been continuing interest in the behavior of shock Hugoniot for high pressures, in particular for particle velocities greater than 10 km/s. Data has been obtained for such mainly through laser and nuclear shock experiments.<sup>1-4</sup> These data, plotted either as shock velocity  $U_s$  of a sample material versus  $U_p$  of an assumed standard material or as  $U_s$  versus  $U_p$  of the sample, are remarkably linear. Modeling, as represented by the SESAME database,<sup>5</sup> shows the same behavior. A general understanding of this linearity and of the Hugoniot as a whole is needed.

## Formalism

Rather than go to detailed, complex modeling I use only the Hugoniot jump conditions and thermodynamics to explain the linear regime. I assumed I have the hydrodynamic equation of state  $P(\rho, E)$  and the three Hugoniot relations

$$P = \rho_o U_s U_p \quad (1a)$$

$$\eta = \rho / \rho_o = U_s / (U_s - U_p) \quad (1b)$$

and 
$$E = \frac{1}{2} P (1 / \rho_o - 1 / \rho). \quad (1c)$$

Starting from an initial point  $\rho_o$ ,  $P_o=0$ , and  $E_o=0$ , and solving  $P(\rho, E)$  and (1c) for  $P(\rho)$  one obtains the pressure versus density principal Hugoniot. Then from (1a) and (1b) follows the  $U_s - U_p$  curve. I proceed by looking at some point 1 on the Hugoniot, shocking from  $\rho_o$ . I expand  $P(\rho, E)$  in a double Taylor series in  $\rho$  and  $E$  around point 1 and solve for the  $U_s - U_p$  Hugoniot near point 1. Then I differentiate the resulting equation with respect to  $U_p$  and evaluate all variables at point 1 to derive an exact relation. The resulting equation can be written as

$$s = 1 + \frac{1}{2}(\gamma - x) + g \quad (2)$$

with  $g = \frac{1}{4}(2 + \gamma + x) \left\{ \left[ 1 + 8x(B_s / P - \gamma - 1) / (2 + \gamma + x)^2 \right]^{\frac{1}{2}} - 1 \right\}$  .

Here,  $x = c / U_p, \gamma = \frac{1}{\rho} \frac{\partial P}{\partial E} \Big|_p$ , and  $\frac{\rho}{P} \frac{\partial P}{\partial \rho} \Big|_E = B_s / P - \gamma$ , where  $B_s = \rho \frac{\partial P}{\partial \rho} \Big|_s$ .

The lower case s is the slope of the local tangent line of the  $U_s - U_p$  curve at  $U_p$  and c is the  $U_p = 0$  intercept of the tangent. All quantities in (2) are on the Hugoniot and thus are to be thought of as functions of  $U_p$  or another Hugoniot variable. This is a fairly complex algebraic relation among s, c,  $U_p, \gamma, P$ , and  $B_s$ , especially with g, but it is quite manageable and we can learn from it.

I look at an interesting and useful aside. From the definition of s,

$$U_s = sU_p + c = \int_0^{U_p} s dU_p + c_o . \quad (3)$$

Substitute (2) in (3) for s and differentiate with respect to  $U_p$  along the Hugoniot. One then obtains a differential equation for c which can be solved to obtain

$$c = -\frac{1}{U_p} \int_0^{U_p} U_p^2 (\gamma^{(1)} + 2g^{(1)}) dU_p , \quad (4)$$

and from (2)  $s = 1 + \gamma / 2 - c / 2U_p + g$ . Either by expanding  $\gamma^{(1)}$  and  $g^{(1)}$  in a Taylor series around  $U_p$  or by integrating by parts, (4) can be re-expressed as

$$c = 2U_p \sum_{n=1}^{\infty} \frac{(-1)^n U_p^n}{(n+2)!} (\gamma^{(n)} + 2g^{(n)}) , \quad (5)$$

where the (n) means n differentiations with respect to  $U_p$  along the Hugoniot.

## Orientation

Before I give results from the above let me present the generic behavior of a metal Hugoniot with only phase transitions with small volume change. I use our latest Mo equation of state (solid line in graphs) as an example.<sup>5</sup> The structures will seem small but this is the reality of  $U_s - U_p$  curves. I look at three figures. In Fig. 1 we see the lower Hugoniot which is given very accurately by two dashed straight lines, one with slope 1.245, the other with 1.196. There is clearly a break at  $U_p \cong 5 \text{ km/s}$ . This is typical for many materials, as it is usually between 3 and 7  $\text{km/s}$ , but the break is a little small because for Mo the lower slope is close to the upper value of 1.196. In other materials, such as in Fig. 4 for iron, the initial slope is larger. Figure 2 shows the next larger scale with the same dashed line fit to the upper part of Fig. 1. From  $U_p \cong 6 \text{ km/s}$  to over 100  $\text{km/s}$  it is an excellent fit. The two chain-dashed lines are straight lines through the origin, the upper with slope 4/3, the lower with slope 1.228. The upper is the ideal gas limit which the physical Hugoniot must ultimately approach. The lower is the lowest slope tangent line to the  $U_s - U_p$  curve that goes through the origin. In such a circumstance  $c = 0$ . Then from (1b)  $\rho$  is not varying so the density derivation of  $P$  is infinite. In my example this point on the Hugoniot is the turnaround point, or point t, and is the maximum density on the Hugoniot. In the case of Mo  $U_{p,t} \cong 262 \text{ km/s}$ . For stronger shocks  $c < 0$  and the density is decreasing as  $U_p$  increases. At any point where  $c = 0$ ,  $P$  has infinite slope and, since  $g_t = x_t = 0$  then from (2)  $s_t = 1 + \gamma_t / 2$ . Also from (1b)  $\rho_t / \rho_o = s_t / (s_t - 1)$ . Typically for many materials  $\rho_t / \rho_o$  ranges between 5 and 6.2 implying  $1.19 \leq s_t \leq 1.25$  and  $0.38 \leq \gamma_t \leq 0.5$ . The slope of the very linear section between  $U_p \cong 10$ , and maybe 100  $\text{km/s}$  or more, ranges between 1.14 and 1.22. Fig. 3 shows an even larger scale and indicates the very slow approach to the ideal gas line of slope 4/3. The Mo Hugoniot is only approaching the ideal gas by  $U_p \cong 2000 \text{ km/s}$ .

## Results

Now follows some analysis using my equation. If one takes the  $U_p \rightarrow 0$  limit of (2), I obtain the very initial slope and curvature of the Hugoniot as the Taylor series  $U_s / c_o = 1 + s_o U_p / c_o + e (U_p / c_o)^2 \dots$ . (One must in all analysis of the formalism carefully expand all quantities self-consistently.) After a few thermodynamic manipulations, I obtain  $s_o = \frac{1}{4} \left[ 1 + \frac{\partial B_s}{\partial P} \right]_s$  and  $e = \left[ 0.5 \rho_o \frac{\partial^2 B_s}{\partial \rho \partial P} \right]_s + s_o (2 + \gamma_o - s_o) / 6$ . The initial slope is directly given by the pressure derivative of the bulk modulus at constant entropy and the curvature is given by the higher constant entropy derivation of the  $B_s$  with  $\gamma_o$  first entering the expansion at this order. It is common, my Mo is an example, that the Hugoniot out to the break is very linear. This form for  $e$  partially explains why. The first term and second terms for  $e$  are dimensionless quantities and thus, in magnitude, should lie between one and ten. The sign of the first is negative, the second positive with resulting cancellation. After dividing by six, one expects  $e$  to be small with resulting linear  $U_s - U_p$ . For Nb I estimate that  $e = 0.16$ .<sup>7</sup> The natural variables that follow from the analysis of (2) for the series are  $U_s / c_o$  and  $U_p / c_o$ , where  $c_o$  is the bulk sound velocity at  $U_p = 0$ . This implies that the break should occur for  $U_p \sim c_o$ . We will see later that  $U_p = 1.6 c_o$  predicts the break quite well.

One can do large  $U_p$  expansions to find the approach to ideal gas. If it is assumed that the Debye-Hückel theory<sup>8</sup> describes the very high temperature gas, for large  $U_p$ ,  $\gamma \sim \frac{2}{3} - b / U_p^3$ ,  $b > 0$ . Then from (2)  $s \sim \frac{4}{3} + a / U_p^2 - 2b / U_p^3$ ,  $c \sim -2a / U_p + 3b / U_p^2$ , and  $P \sim 12 \rho_o a / (\rho / \rho_o - 4)$  with  $a > 0$ . The parameter  $a$  is given by the sum of cohesive, ionization, and dissociation energies in going from ambient to  $T \rightarrow \infty$ .

I can expand around point  $t$  and find the curvature. Letting  $U_s = s_t U_p + \alpha_t (U_p - U_{p,t})^2$ ,  $\alpha_t$  is given by  $\alpha_t = \gamma_t^{(1)} (1 + \gamma_t / 2) / (2 B_{s,t} / P_t - \gamma_t)$ . It is a good approximation that  $\alpha_t = \gamma_t^{(1)} / 2$ . Using numbers from the Mo equation of state  $\alpha_t \sim 10^{-4} \text{ s/km}$  and  $U_s$  is well approximated by the quadratic form for  $|U_p - U_{p,t}| \lesssim 100 \text{ km/s}$ .



At this point I already have an argument for the  $U_s - U_p$  curve to be very linear for  $10 \lesssim U_p \lesssim 200 \text{ km/s}$  or even higher. There has to be an inflection point between 10 and 262 km/s. I estimate for Mo from (2) that it is at  $U_p \cong 125 \text{ km/s}$ . There  $\alpha$  is zero and should continue for smaller  $U_p$  being small and negative. (Think of a Taylor series around the inflection point.) Thus the curvature is very small and the curve is close to linear. I actually did not even need to estimate  $\alpha_t$  because the slow approach of the  $U_p - U_p$  curve to the ideal gas behavior implies it is small.

But I can go into more detail with (2). For that I need the qualitative behavior of  $\gamma$  and  $g$  as functions of  $U_p$  which is obtained from the SESAME database where the relevant physics comes from either TFD models or the Inferno model.<sup>9,10</sup> The two models are compatible to the level I need and one can see that the predicted features of  $\gamma$  and  $g$  are physical. At low  $U_p$ ,  $\gamma$  is high, say 1.5. For  $U_p$  between 3 and 7 km/s, the temperature between  $10^4$  and  $3 \times 10^4$  K,  $\gamma$  drops fairly rapidly toward 0.4. Once  $U_p$  is greater than 7 km/s or so,  $\gamma$  goes through a very broad minimum with  $\gamma^{(1)}$  being very small. Ultimately, at large  $U_p$ ,  $\gamma$  slowly rises to go to the ideal gas limit of  $2/3$ . The physics of the decline of  $\gamma$  is that the electronic thermal excitations are starting to dominate the equation of state at the  $U_s - U_p$  breakpoint. They pull  $\gamma$  down below the ideal gas value through the region the electrons are ionizing. For small  $U_p$ ,  $g$  diverges as  $1/U_p$  but as  $U_p$  increases  $g$  is decreasing so that by  $U_p \cong 10 \text{ km/s}$ ,  $g \cong 1/6$ . For larger  $U_p$ ,  $g$  continues to smartly decrease because it is proportional to both  $x$  and  $B_s / P - \gamma - 1$  which are both getting small. The  $g$  is correspondingly small.

The physics of all this is that for smaller  $U_p \lesssim 7 \text{ km/s}$  the equation of state is dominated by the zero temperature isotherm and the phonons. Here  $g$  is large. As  $U_p$  increases and goes through the break the thermal excitations, the electrons, come into play pulling down  $g$  until it can be dropped from the picture. This allows  $\gamma$  to determine  $s$  and the electrons are pulling  $\gamma$  down toward 0.4. All this causes the break. Putting this together in (2) or (4) and (5) I conclude that  $s$  is well approximated by  $s = 1 + \gamma/2$  for  $U_p$  from just above the

break at  $3-7 \text{ km/s}$  to well above the turnaround. With  $\gamma \cong 0.4$ ,  $s \cong 1.2$  for the region between 10 and  $100 \text{ km/s}$ , which is quite in line with my earlier statement of between 1.14 and 1.22.

### Experimental Comparison

All of what I have said fits very well with the detailed modeling that goes into the SESAME database, both TFD and Inferno. It also agrees very well with experiments Figure 4 shows data for iron and two straight line, least-square fits to the upper and lower portions of the data. I do not show all the lower data as it then would be too dense; it is very linear with a fitted slope of 1.553. The other line, fitted to the upper five points, has a slope of 1.213, in excellent agreement with all I have said. The uppermost data point, one point of the pair next down, and the fourth and sixth points down are absolute measurements. The other two high  $U_p$  points are measured assuming lead as a standard. The error bars on the uppermost point are  $\pm 2\%$  in both  $U_p$  and  $U_s$ . The high  $U_p$  data and some of the low  $U_p$  come from the Russian literature.<sup>11</sup> The rest of the low data is from the Los Alamos Shock Compendium.<sup>12</sup>

I have also looked at Cu, Bi, Sn, Ar, Xe and Al which all show the break with slopes above it of 1.170, 1.203, 1.162, 1.144, 1.166 and 1.149, respectively.<sup>12,13,14</sup> These data do not go to as high a  $U_p$  as that of the iron, but they do strongly support the existence of the break and the linearity.

I look now to the break and define it by the intersection of the linear fits to the higher and lower portions of the  $U_s - U_p$ . In Fig. 5 I plot the location of the break as a function of  $c_o$  for Al, Fe, Cu, Sn, Bi, Ar, and Xe, going down from the highest points to the lowest. The solid curve is a fit with a straight line through the origin; the slope is 1.6.

There are data on  $N_2$ , a molecular system, which show a break and also there is modeling showing a negative  $\gamma$  in the dissociation region.<sup>14,15</sup> I am pushing a little to compare here but the slope above the break is 0.985 and  $\gamma=-0.03$ . The dissociation pulls

the  $\gamma$  down lower than ionization.

## Shell Structure

I now discuss the effect of shell structure on the Hugoniot above the break. Here shell structure enters in two ways. One is through the variation in  $\rho_o$  in going through the periodic table. This in particular varies the location of the turnaround point. But I do not want to focus on this. I look to the shell structure from the thermal part of the equation of state. I obtain upper bounds on the variation of  $\gamma$  and  $g$  due to shell structure from Inferno. I see no shell structure in  $B_s / P - \gamma$ , and, as this is a density derivative, this makes sense. So I drop  $g$  from the equations and I can argue that this is a conservative approximation for the size of the variation in  $s$ . For Al and higher atomic numbers the maximum variation in  $\gamma$  is  $\pm 0.1$ , with a functional form that is quadratic in  $\ln U_p$  and a width guided by Inferno.

From (2) the variation in  $s$  is  $\Delta s = (\Delta\gamma - \Delta c / U_p) / 2$ . From (4) I have  $\Delta c$  in terms of  $\Delta\gamma^{(1)}$ . So one finds the variation in  $s$ , but what is of interest is  $\Delta U_s$  which is an integral of  $\Delta s$ . Carrying all this out I find that for the  $\pm 0.1$  in  $\gamma$ ,  $U_s$  varies by  $\pm 2\%$ , quite in line with what is seen in full SESAME equations of state based on Inferno. These are conservative approximations and this is a maximum variation at an exact  $U_p$ . It will be extremely difficult to see shell structure above the break. If one goes to the  $P(\rho)$  Hugoniot and looks in the neighborhood of the turnaround, the small wiggles in  $U_s$  are amplified by the presence of the singularity and appear large. But experiments are not known that can measure  $P$  and  $\rho$  directly, so this is not relevant.

## Summary

I have presented a number of results. First is (2) which relates Hugoniot variables and thermodynamic quantities. From it I have expansions of the Hugoniot for  $U_p \rightarrow 0$ ,  $U_p \rightarrow \infty$ , and  $U_p$  at turnaround. From simple features of the equation of state the linear region above the break is understood and the slope and location of the break are estimated. The pertur-

bation of thermal shell structure is quantified.

I have focused in this paper on elemental metals and certainly I feel the ideas are valid there. (I am not referring here to the exact results, such as (2), but to the approximate.) For all other substances, if one is high enough up the Hugoniot that all molecules are dissociated, then all should be applicable. Further down, the details of my picture will be altered for molecular systems and insulators. An example here is the  $N_2$ . Furthermore, below the break where the thermal no longer dominates, phase transitions with larger volume change introduce structure. Also, for the alkali metals there are shell structure affects for small  $U_p$ . But even with these caveats I have a very powerful overview.

#### Acknowledgment

I wish to thank all my friends, from minor acquaintances to those closest to me, for putting up with me through this project. This work was supported by the U.S. Department of Energy under contract number W-7405-ENG-36.

## References

- (1) C. E. Ragan III, Phys. Rev. A 29, 1391 (1984) and references therein.
- (2) W. J. Nellis, J. A. Moriarty, A. C. Mitchell, M. Ross, R. G. Dandrea, N. W. Ashcroft, N. C. Holmes, and G. R. Gathers, Phys. Rev. Lett. 60, 1414 (1988).
- (3) R. Cauble, D. W. Phillion, T. J. Hoover, N. C. Holmes, J. D. Kilkenny, and R. W. Lee, Phys. Rev. Lett. 70, 2102 (1993).
- (4) M. Koenig, B. Faral, J. M. Boudenne, D. Batani, A. Benuzzi, S. Bossi, C. Rémond, J. P. Perrine, M. Temporal, and S. Atzeni, Phys. Rev. Lett. 74, 2260 (1995).
- (5) S. P. Lyon and J. D. Johnson, Sesame: Los Alamos National Laboratory Equation of State Database, Los Alamos Report No. LA-UR-92-3407, 1992 (unpublished).
- (6) See, for example, J. O. Hirschfelder, C. F. Curtiss, and R. B. Bird, Molecular Theory of Gases and Liquids ( John Wiley and Sons, Inc., New York, 1954).
- (7) I thank J. Wills for furnishing me with an estimate of the double derivation of  $B_S$  for Nb.
- (8) L. D. Landau and E. M. Lifshitz, Statistical Physics (Addison-Wesley Publishing Company, Reading, 1969).
- (9) R. D. Cowan and J. Ashkin, Phys. Rev. 105, 144 (1957).
- (10) D. A. Liberman, Phys. Rev. B 20, 4981 (1979).
- (11) L. V. Al'tshuler, A. A. Bakanova, I. P. Dudoladov, E. A. Dynin, R. F. Trunin, and B. S. Chekin, J. Appl. Mech. Mech. Techn. Phys. 22, 145 (1981); L. V. Al'tshuler and B. S. Chekin, in Proceedings of First All-Union Pulsed Pressures Symposium, VNIIFTRI, Moscow, 1974 (unpublished); L. V. Al'tshuler, N. N. Kalitkin, L. V. Kuz'mina, and B. S. Chekin, Sov. Phys.-JETP 45, 167 (1977); R. F. Trunin, M. A. Produrets, L. V. Popov, V. N. Zubarev, A. A. Bakanova, V. M. Ktitorov, A. G. Sevast'yanov, G. V. Simakov, and I. P. Dudoladov, Sov. Phys.-JETP 75, 777 (1992); R. F. Trunin, M. A. Podurets, B. N. Moiseev, G. V. Simakov, and A. G. Sevast'yanov, Sov. Phys.-JETP 76, 1095 (1993); and references therein.
- (12) LASL Shock Hugoniot Data, edited by S. P. Marsh (University of California Press, Berkeley, 1980).
- (13) See Ref. 10. Also, S. B. Kormer, A. I. Funtikov, V. D. Ulrin, and A. N. Kolesnikova, Sov. Phys.-JETP 15, 477 (1962); B. L. Glushak, A. P. Zharkov, M. V. Zhernokletov, V. Ya. Ternovoi, A. S. Filimonov, and V. E. Fortov, Sov. Phys.-JETP 69, 739 (1989); M. V. Zhernokletov, V. N. Zubarev, and Yu. N. Sutulov, Zh. Prikl. Mekh. Tekhn. Fiz. 1, 119 (1984); L. P. Volkov, N. P. Voloshin, A. S. Vladimirov, V. N. Nogin, and V. A. Simonenko, Sov Phys.-JETP Lett. 31, 588 (1980); V. A. Simonenko, N. P. Voloshin, A. S. Vladimirov,

- A. P. Nagibin, V. P. Nogin, V. A. Popov, V. A. Sal'nikov, and Yu. A. Shoidin, *Sov. Phys.-JETP* 61, 869 (1985); and E. N. Avrorin, B. K. Vodolaga, N. P. Voloshin, V. F. Kuropatenko, G. V. Kovalenko, V. A. Simonenko, and B. T. Chernovolyuk, *Sov. Phys.-JETP Lett.* 43, 308 (1986).
- (14) W. J. Nellis and A. C. Mitchell, *J. Chem. Phys.* 73, 6137 (1980) and W. J. Nellis, M. van Thiel, and A. C. Mitchell, *Phys. Rev. Lett.* 48, 816 (1982).
- (15) W. J. Nellis, H. B. Radousky, D. C. Hamilton, A. C. Mitchell, N. C. Holmes, K. B. Christiansen, and M. van Thiel, *J. Chem. Phys.* 94, 2244 (1991) and H. B. Radousky, W. J. Nellis, M. Ross, D. C. Hamilton, and A. C. Mitchell, *Phys. Rev. Lett.* 57, 2419 (1986).

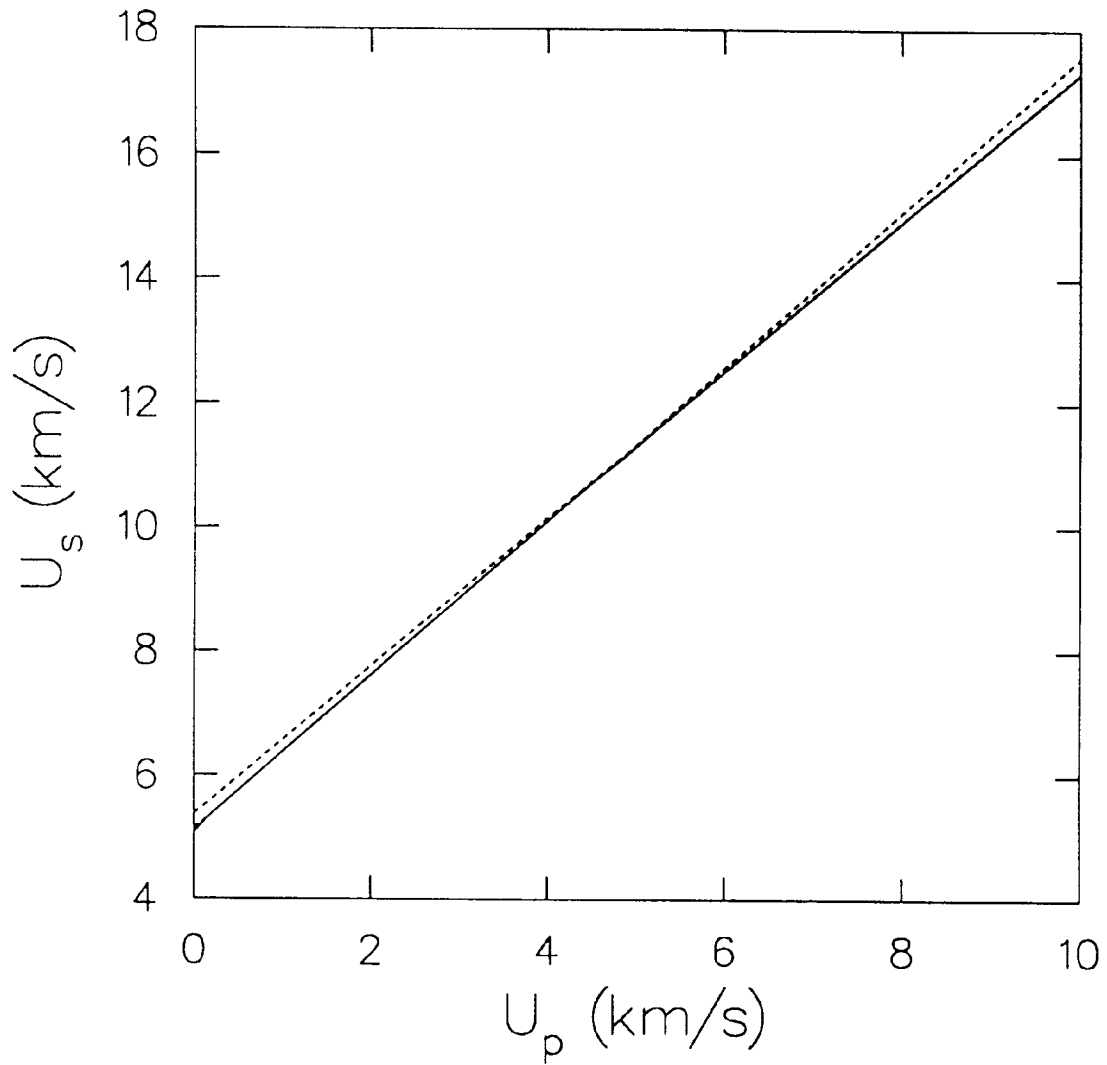


Fig. 1. Mo Hugoniot - lower portion around break. The solid line is the Mo Hugoniot. The two dashed lines are straight line fits to the two linear portions of the Hugoniot.

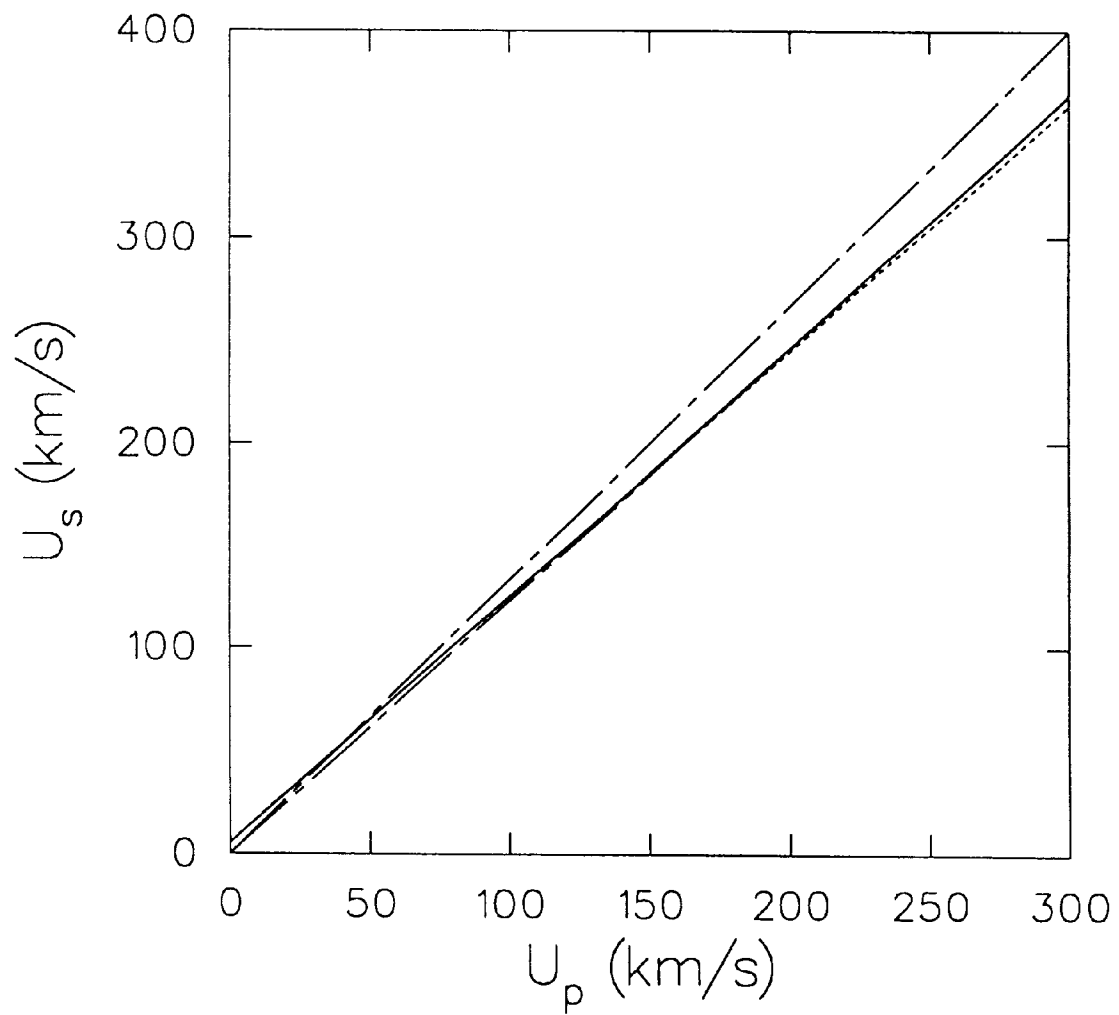


Fig. 2. Mo Hugoniot -  $U_p$  out to turnaround. The dashed line is from the fit above the break. It shows that the straightness of the solid Hugoniot curve persists to quite high  $U_p$ .



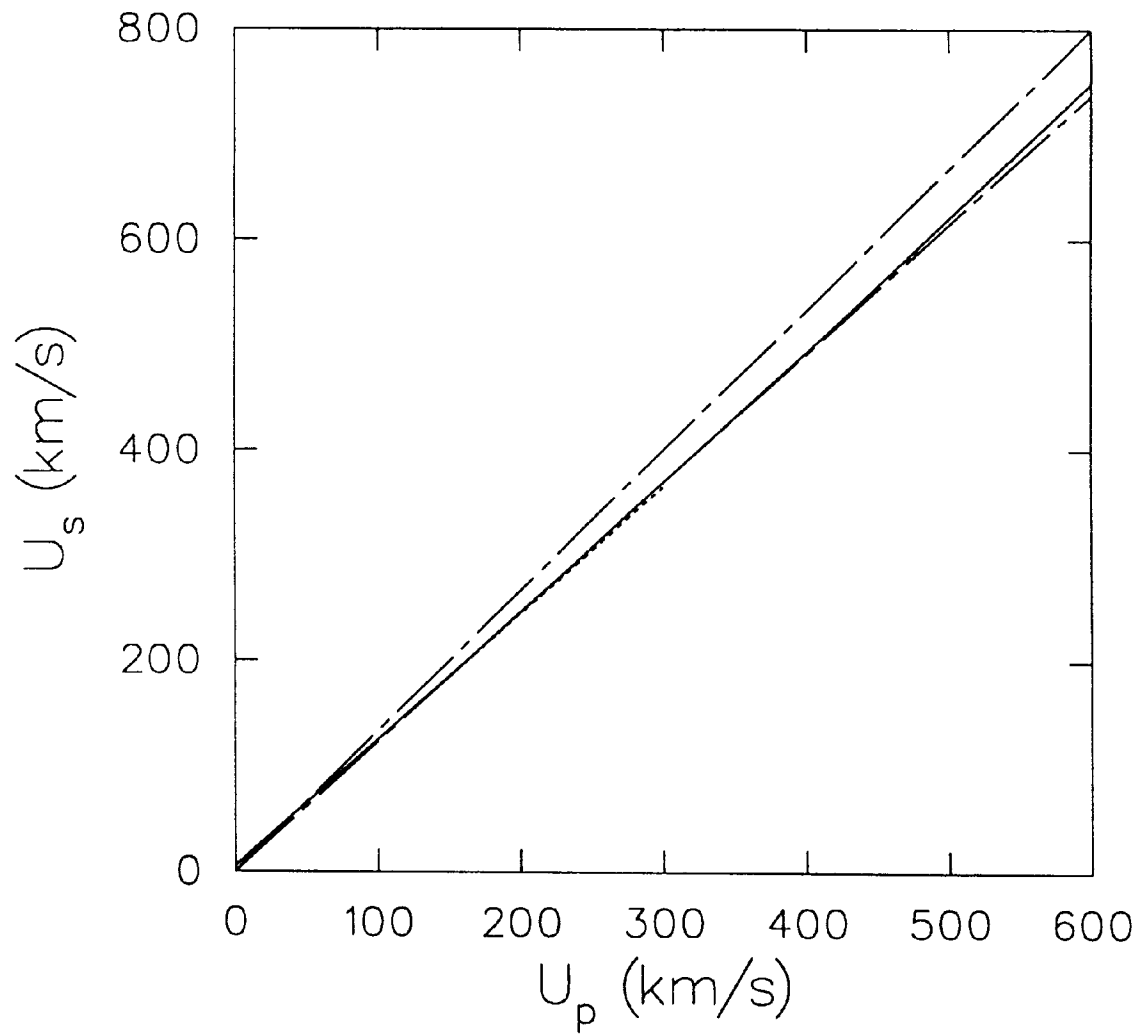


Fig. 3. Mo Hugoniot - a still larger view with the turnaround point and the slow approach to ideal gas. Curves are the same as Fig. 2.

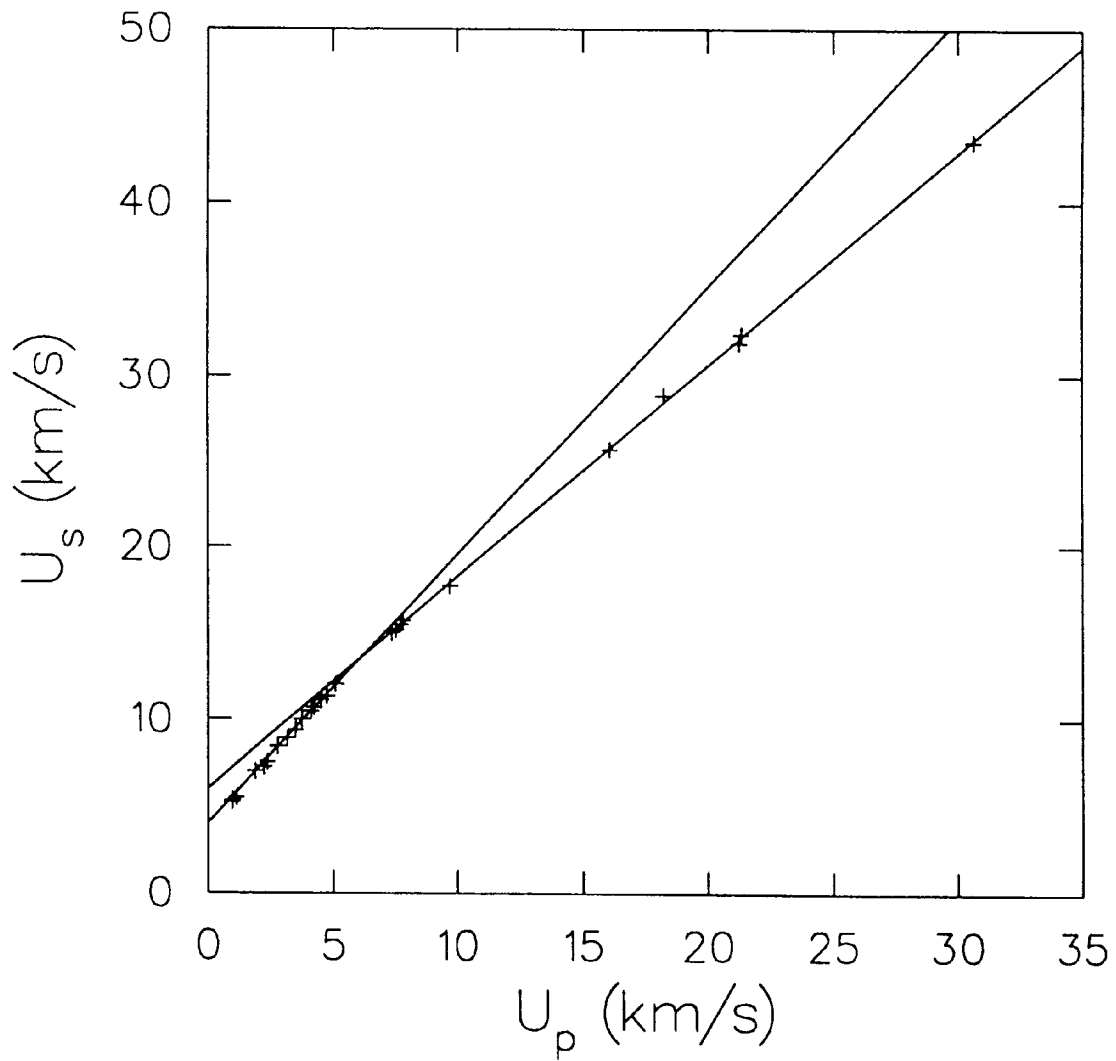


Fig. 4. Fe Hugoniot data. We see clearly the linearity of the upper data and a well defined break.

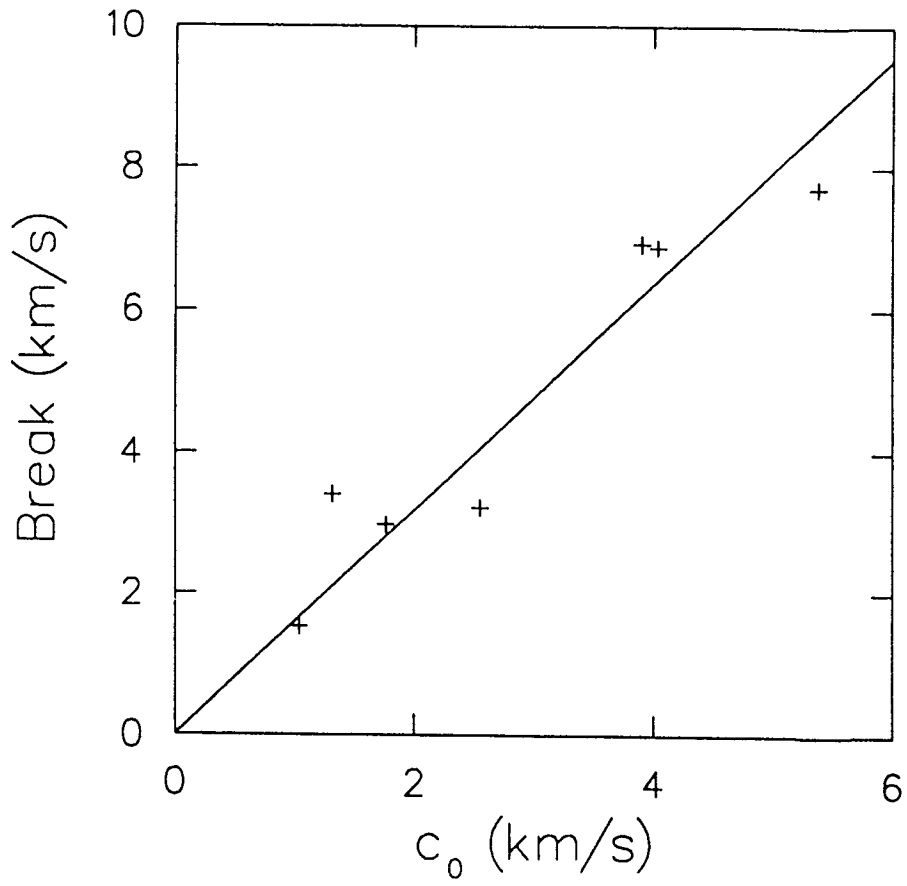


Fig. 5 Breakpoint as a function of  $c_0$ .

